Technical University of Denmark

DTU

Gliding arc surface modification of carrot nanofibre coating - perspective for composite processing

Kusano, Yukihiro; Berglund, L; Aitomäki, Y; Oksman, K; Madsen, Bo

Link back to DTU Orbit

DTU Library
Technical Information Center of Denmark

Gliding arc surface modification of carrot nanofibre coating – perspective for composite processing

Y Kusano[1], L Berglund[2], Y Aitomäki[2], K Oksman[2] and B Madsen[1]

[1]Department of Wind Energy, Section of Composites and Materials Mechanics, Technical University of Denmark, Risø Campus, DK-4000 Roskilde, Denmark
[2]Division of Materials Science, Composite Centre Sweden, Luleå University of Technology, SE-971 87 Luleå, Sweden

E-mail: yuki@dtu.dk

Abstract. Surfaces of carrot nanofibre coatings were modified by a gliding arc in atmospheric pressure air. The treatment strengthened wetting of deionized water and glycerol, increased an oxygen content, C-O and C=O, and moderately roughened the surfaces. In the perspective of composite materials, these changes to the nanofibres can potentially improve their processability when they are to be impregnated with a polymeric matrix. However, longer exposure to the gliding arc reduced oxidation and roughness of the surface, and thus there exists an optimum condition to achieve good wetting to solvents.

1. Introduction

Non-thermal plasma processing at atmospheric pressure is widely used for surface modification [1, 2]. Its applications include surface cleaning [3], decontamination and sterilization [4,5], deposition of functional coatings [6], and improvement of adhesion, wetting and paintability [7-15].

One of the challenges in non-thermal plasma processing at atmospheric pressure is to achieve high reactivity and high productivity simultaneously [16]. Here, high reactivity is ensured by a high electron temperature in a non-equilibrium plasma so as to change chemical bonding of molecules in the plasma or the plasma-treated surfaces. Meanwhile, high productivity can be demonstrated using high energy densities. However, most plasmas can hardly sustain a non-equilibrium state at high energy densities. One possible approach to overcome this issue is to develop a hybrid plasma with a high energy density in a non-equilibrium state.

A gliding arc is one of the hybrid plasmas [17], generated between diverging electrodes as a low-impedance thermal arc discharge, extended by a gas flow and quenched to a non-thermal condition [18]. It can be operated in atmospheric pressure air and thus advantageously used for large-scale processing [19-26]. An alternating current (AC) gliding arc has a long lifetime extending over hundreds of AC periods without extinction. The plasma column can be elongated to approximately 20 – 30 cm [21-29]. The AC gliding arc is useful for adhesion improvement of glass fibre reinforced polyesters (GFRPs) [22,23], efficiently oxidizing GFRP surfaces when the distance between the edge of the electrodes and the GFRP surface is up to 6 cm in open air. It is also demonstrated that optical techniques are promising for non-instructive diagnostics of the AC gliding arc [24-29]. In particular, the dynamics of the gliding arc is observed by using a high-speed camera. In addition, excited and ground-state hydroxyl radicals are observed in the plasma column and its vicinity, respectively. It is

noted that the hydroxyl radical has a high oxidation potential, next to fluorine and higher than ozone and chlorine. Therefore, the hydroxyl radicals generated by the gliding arc can play an important role in surface modification.

Cellulose is renewable, nontoxic, and biodegradable, and is known to be the most abundant biopolymer on earth [30]. It has been extensively studied in terms of biological, chemical, and mechanical properties. In particular, nano-celluloses (NCs) have attracted significant interests due to their high strength, high modulus, high surface area and unique optical properties. Typical lateral dimensions are approximately 5 – 20 nm, while longitudinal dimensions are from tens of nm to several μm [31]. Acid hydrolysis of cellulose will remove the amorphous part of cellulose and lead to highly crystalline and rigid nanoparticles called cellulose nanocrystals or cellulose nanowhiskers [32]. On the other hand, cellulose nanofibres (CNF) can be produced by ultrafine grinding, microfluidization or high pressure homogenization through delamination of fibre cell walls and subsequent liberation of nano-sized fibrils [33].

Promising application for demonstrating mechanical properties of NCs is to mix NCs to impregnate a nanofibre network with a polymer and create strong, light-weight and transparent composite [34]. Its application includes packaging [35,36], vehicles and aeronautical applications. For demonstrating the best performance of NC composites, it is important to achieve substantial dispersion of NCs and strong interfacial interaction between the NC and the polymer matrix. In this respect, surface modification of NCs has attracted significant interests [37,38].

However, surface modification of NCs is not an easy task even using a plasma. For example, when NC is dispersed in a liquid, a plasma as a gas phase does not have a direct contact with NC surfaces. On the other hand, when NCs are dried without a liquid, they are easily aggregated, disturbing uniform surface treatment. There are some studies presented in literature to solve or tackle with these handling problems [1].

In the present work, as a feasibility study, effects of plasma treatment on NC are investigated in a simplified form of NC so as to avoid the above handling problems. That is, nanofibre coatings are treated by a plasma not because of the application for coatings, but because of a simplified specimen feature. More specifically, nanofibres were separated from a carrot residue, dispersed in water, painted on a glass plate, and dried. The subsequent coating surfaces were treated using a gliding arc in atmospheric pressure air. The treated surfaces were characterized by means of contact angle measurements, x-ray photoelectron spectroscopy (XPS), and field emission scanning electron microscopy (FE-SEM) in order to investigate the treatment effect.

2. Experimental methods

2.1 Materials

Carrot nanofibres were isolated from carrot residue supplied by Brämhults Juice AB, Sweden. This raw material is a by-product from carrot juice production. A chemical purification was carried out prior to the fibrillation following the procedure described by Siqueira et al. (2016) [31]. The residue was first washed with distilled water at 85°C, alkali-treated (2% NaOH) at 80°C for 2h, and subsequently bleached with $NaClO_2$ (1.7 %) in an acetic buffer (pH 4.5) at 80°C for 2h for lignin removal. Finally the material was washed until a neutral pH was reached.

This bleached residue was fibrillated by ultrafine grinding using a supermass colloider (MKZA10-20J, Masuko Sangyo, Japan), at consistency of 2%. Prior to the grinding, the suspension was dispersed using a shear mixer (Silverson L4RT Silverson Machine Ltd., England). The grinding was operated at a rotor speed of 1,500 rpm and the grinding stones were gradually adjusted to 100 μm (negative). The total processing time was 40 min. The obtained aqueous carrot nanofibre suspension (2wt% concentration) was used to prepare coatings on glass plates (CORNING® 2947-75x25), and dried at room temperature in atmospheric pressure air for a couple of days. The coating thickness was estimated to be approximately 6 μm.

2.2 Plasma treatment

The gliding arc was generated between two diverging stainless steel tubular electrodes as shown in Figure 1. The outer diameter of the tubular electrodes is 3 mm. Cooling water was fed through the electrodes during operation [22-29]. An air flow was fed between the electrodes with a flow rate of 17.5 standard litres per minutes (SLM). The gliding arc was driven by an AC power supply at a frequency of 31.25 kHz (Generator 6030, SOFTAL Electronic GmbH). The electric power applied to the gliding arc was approximately 700 W. In order to treat the nanofibre coating surface without excess thermal damage from the gliding arc, a poly(methyl-methacrylate) holder was moved forward and backward at a speed of 180 mm/s on which the coated glass plate was fixed. The angle between the gas flow direction and the specimen surface is approximately 90º when the surface is treated. The closest distance between the coating surface and the edges of the electrodes was 15 mm.

Figure 1. A photo of the gliding arc with water cooled electrodes.

2.3 Surface characterization

Surface characterization is vitally important to understand the surface modification effects and to optimize the process conditions.

Contact angles were measured with deionized water and glycerol in air at room temperature both before and after the gliding arc treatment using a contact angle measurement system (CAM100, Crelab Instruments AB, Sweden). A typical drop size was $1\mu L$. The contact angle was measured within 5 s after the drop was attached onto the surface. Typically 10 measurements were made for each specimen, and their arithmetic mean was calculated.

XPS data were collected using a micro-focused, monochromatic Al Kα X-ray source (1486.6 eV) with a lateral resolution of 30 μm (K-alpha, ThermoFischer Scientific, UK). Atomic concentrations of

all elements were calculated by determining the relevant integral peak intensities using the Shirley background. The K-alpha was also used for a high resolution analysis on the carbon 1s (C1s) spectra acquired over 30 scans. The binding energies were referred to the hydrocarbon component ($\underline{C}$-H, $\underline{C}$-C) at 285 eV. The spectra were de-convoluted through curve fitting, taking purely Gaussian components with linear background subtraction. The full-width at half-maximum (FWHM) for all peaks of C1s was constrained to 1.5 eV.

The surface morphology of the nanofibre coating was observed by using an FE-SEM (Zeiss SUPRA 35, Germany). The NFC surfaces were sputter-coated with approximately 15-nm thick Au before the observation.

3. Results and discussion

The contact angles of the nanofibre coating were measured before and after the gliding arc treatment. Typical images of the deionized water- and glycerol-drops on the nanofibre coatings are shown in Figure 2.

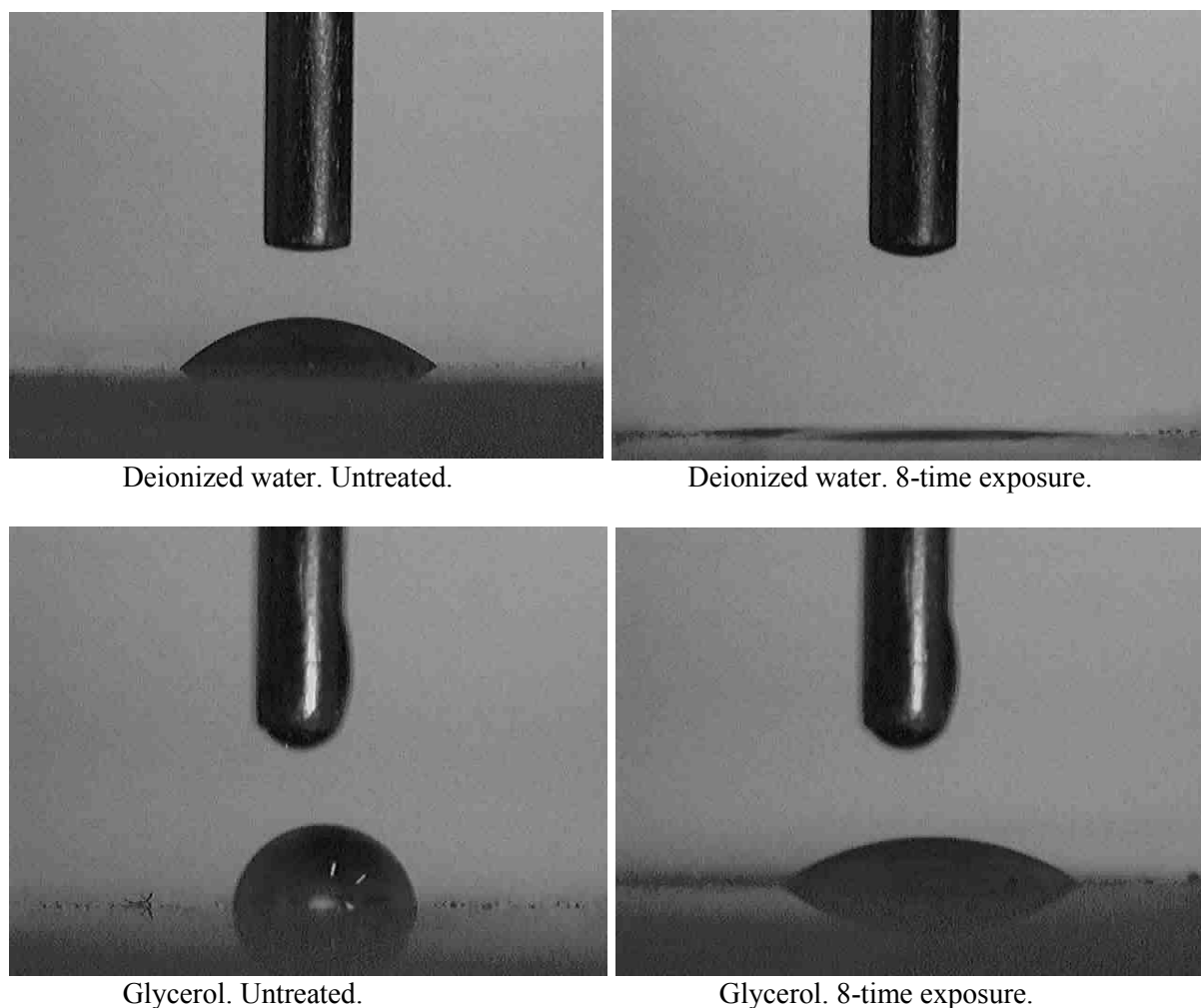| Deionized water. Untreated. | Deionized water. 8-time exposure. |
| Glycerol. Untreated. | Glycerol. 8-time exposure. |

Figure 2. Typical photo images of deionized water-drops and glycerol-drops on the nanofibre coatings.

Figure 3 shows measured contact angles of deionized water and glycerol at different numbers of

exposure. The contact angles of deionized water and glycerol before the gliding arc treatment, corresponding to 0-time exposure, were typically between 20º - 35º and 70º - 80º, respectively. The deionized water contact angles tend to decrease as the number of exposure increases, approaching 0º. The glycerol contact angles also tend to decrease as the number of exposure increases, approaching approximately 30º. Enhancement of glycerol wetting is preferable when nanofibres are mixed in a composite, since nanofibres are usually dispersed in an organic solvent for mixing it into a polymeric matrix, potentially improving processability and mechanical properties of the composite. However, it is noted that after 16-time exposure, contact angles of deionized water and glycerol slightly increased.
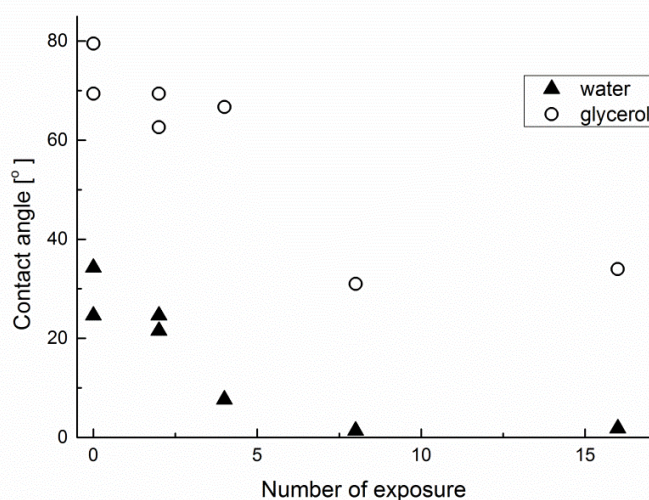

Figure 3. Contact angles of the nanofibre coatings at different times of exposure to the gliding arc. The numbers of exposure are 0 (corresponding to an untreated surface), 2, 4, 8 and 16. Solid triangle: deionized water. Open circle: glycerol.

XPS measurement was carried out to analyze the elemental composition of the nanofibre coatings before and after the gliding arc treatment. The nanofibre surfaces typically contain C, O, Ca, and low concentration impurities. The atomic ratios of O/C and Ca/C calculated using the XPS survey spectra are shown in Figure 4 (a). After 2-time exposure, the O/C ratio increased from 0.59 to approximately 0.72. The O/C ratio may not significantly increase by further exposure, and eventually decreased to approximately 0.64 after 16-time exposure. The Ca/C ratio also increased, after the gliding arc treatment, from 0.02 to 0.03-0.04. The increase in the calcium content can be interpreted as preferential etching of organic components in the coatings. It is indicated that the Ca/C ratio does not monotonically increase as the increase in the exposure to the gliding arc, and that the preferential etching of organic component is not a leading effect of the gliding arc treatment.

Deconvolution of the C1s spectra of the nanofibre coatings before and after the gliding arc treatment was carried out. The result is shown in Figure 4 (b). Peaks at approximately 285 eV, 286.8 eV, and 288.4 eV can be assigned to C-H/C-C, C-O, and C=O (carbonyl). A peak corresponding to carboxy group at approximately 289.5 eV was not detected. Since general plasma treatment can readily create carboxy group on polymer surfaces by oxidation [11], it is suggested that the gliding arc may result in moderate oxidation on polymer surfaces. After 2-time exposure, the peak corresponding to C-H/C-C decreased, while then peaks corresponding to C-O and C=O increased. Similar to the O/C ratio, they may not significantly change by further exposure, and after 16-time exposure, the peak of C-H/C-C increased and the peaks of C-O and C=O decreased.
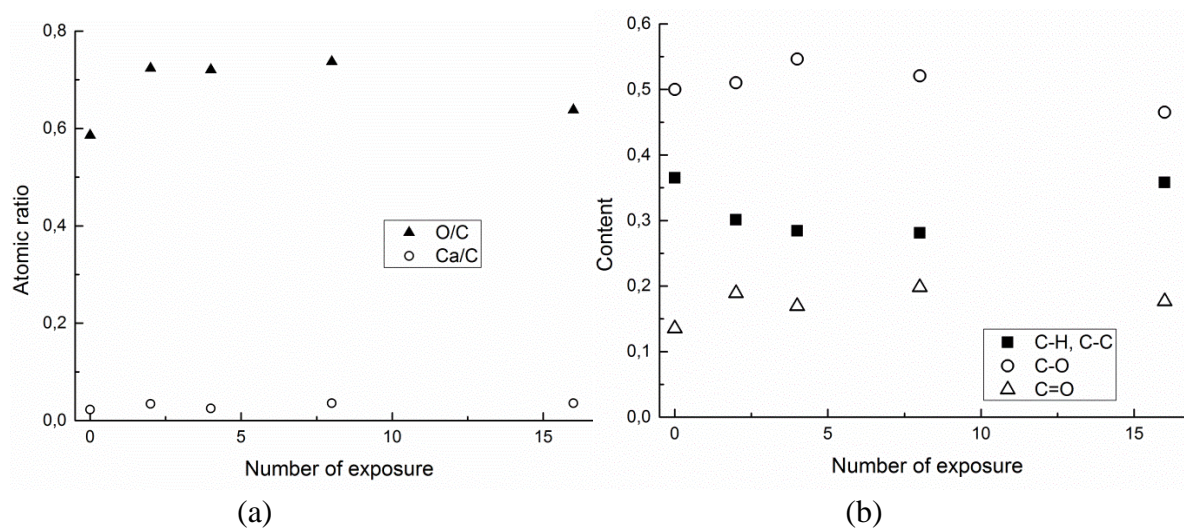
(a)   (b)

Figure 4. (a) O/C and Ca/C ratios of the nanofibre coating surfaces at different times of exposure to the gliding arc. (b) Contents of peaks obtained by curve-fitting of C1s spectra of the nanofibre coating surfaces at different times of exposure to the gliding arc.
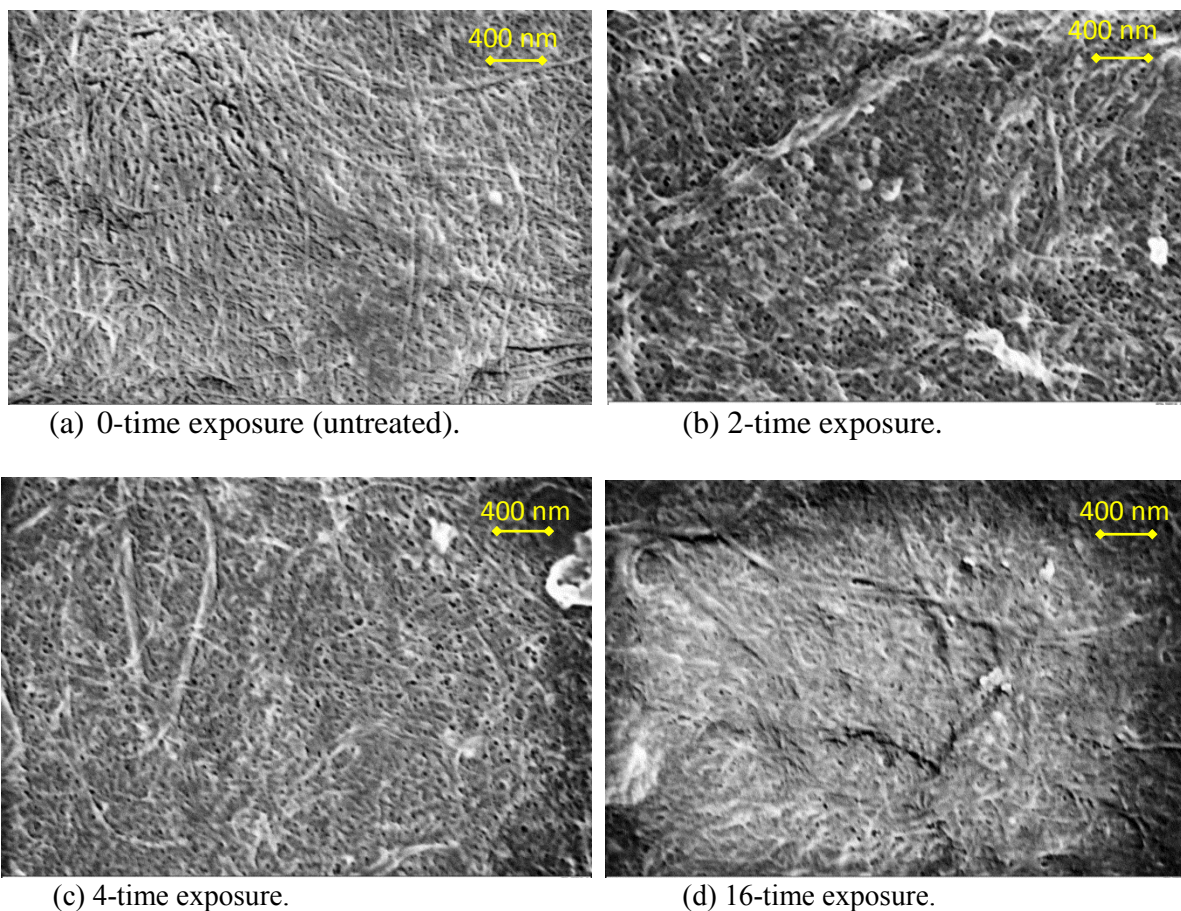

(a) 0-time exposure (untreated).   (b) 2-time exposure.

(c) 4-time exposure.   (d) 16-time exposure.

Figure 5. FE-SEM images of the nanofibre coating surfaces.

The morphological changes after the gliding arc treatment is possible only when nano-scale observation is performed, since plasma surface treatment generally changes the top layer up to 10 nm or less [11]. Figure 5 shows FE-SEM images before and after the gliding arc treatment. Figure 5 (a) indicates that the untreated nanofibre coating shows assemblies of nano-cellulose fibrils surrounded by an unstructured phase. 2-time exposure in Figure 5 (b) seems to roughen the surface, most likely due to the preferential etching of the surrounding phase, supported by the XPS result of the increase in the Ca/C ratio. However, further exposure may not significantly roughen the nanofibre coating surfaces in a nano-scale as shown in Figure 5 (c) and (d). Instead, these images indicate that the surface become smoother in nanoscale, while a larger scale deformation might occur (Figure (d)). A possible explanation of this morphological change by the gliding arc treatment is that the nanofibre coating surface could be etched and roughened moderately, and that longer exposure could result in microscale melting at the surface. A similar phenomenon was observed for the gliding arc treatment of glass-fibre reinforced polyester plates [19].

In next steps, treatment optimisation and treatment of larger amounts of nanofibres will be investigated so as to be feasible for production of carrot nanofibre composites with desired properties.

4. Conclusion
Gliding arc treatment can oxidize and roughen the carrot nanofibre surface and strengthen the wetting of deionized water and glycerol, and thus can be potentially useful for surface modification of the carrot nanofibres when they are mixed in a composite since the treatment can potentially improve processability and mechanical properties of the composite.

Acknowledgement

References
[1]   2011 *Generation and applications of atmospheric pressure plasmas* ed M Kogoma, M Kusano and Y Kusano (New York: NOVA Science Publishers, Inc.) chapters 3-6 pp 45-100
[2]   Kogelschatz U 2003 *Plasma Chem. Plasma Proc.* **23(1)** 1-46
[3]   Yi CH, Lee YH and Yeom GY 2003 *Surf. Coat. Technol.* **171** 237-240
[4]   Leipold F, Kusano Y, Hansen F and Jacobsen T 2010 *Food Control* **21(8)** 1194-1198
[5]   Leipold F, Schultz-Jensen N, Kusano Y, Bindslev H and Jacobsen T 2011 *Food Control* **22(8)** 1296-1301
[6]   Nwankire CE, Favaro G, Duong Q-H and Dowling DP 2011 *Plasma Proc. Polym.* **8** 305-315.
[7]   1994 *Plasma surface modification of polymers: relevance to adhesion* ed M Strobel, CS Lyons and KL Mittal (Utrecht, VSP)
[8]   Kusano Y, Andersen TL and Michelsen PK 2008 *J. Phys. Conf. Series.* **100** 012002
[9]   Kusano Y, Teodoru S and Hansen CM 2011 *Surf. Coat. Technol.* **205** 2793-2798
[10] Singh SV, Kusano Y, Morgen P and Michelsen PK 2012 *J. Appl. Phys.* **111** 083501
[11] Kusano Y 2014 *J. Adhesion* **90(9)** 755-777
[12] Teodoru S, Kusano Y, Rozlosnik N and Michelsen PK 2009 *Plasm. Proc. Polym.* **6** S375-S381
[13] Kusano Y, Mortensen H, Stenum B, Kingshott P, Andersen TL, Brøndsted P, Bilde-Sørensen JB, Sørensen BF and Bindslev H 2007 *Plasm. Proc. Polym.* **4(S1)** S455-S459
[14] Kusano Y, Mortensen H, Stenum B, Goutianos S, Mitra B, Ghanbari-Siahkali A, Kingshott P, Sørensen BF and Bindslev H 2007 *Int. J. Adhesion and Adhesives* **27(5)** 402-408
[15] Lee BJ, Kusano Y, Kato N, Naito K, Horiuchi T and Koinuma H 1997 *Jpn. J. Appl. Phys.* **Pt. 1, 36** 2888-2891
[16] Kusano Y 2009 *Surf. Eng.* **25(6)** 415-416
[17] Fridman A, Nester S, Kennedy LA, Saveliev A and Mutaf-Yardimci O 1999 *Prog. Energy*

   Combustion Sci. **25** 211-231

[18] Czernichowski A 1994 *Pure Appl. Chem*. **66(6)** 1301-1310

[19] Kusano Y, Teodoru S, Leipold F, Andersen TL, Sørensen BF, Rozlosnik N and Michelsen PK 2008 *Surf. Coat. Technol*. **202** 5579-5582

[20] Kusano Y, Norrman K, Drews J, Morgen P, Leipold F, Singh SV, Bardenshtein A and Krebs N 2011 *Surf. Coat. Technol*. **205** S490-S494

[21] Kusano Y, Andersen TL, Toftegaard HL, Leipold F, Bardenshtein A and Krebs N 2014 *Int. J. Mater. Eng. Innovation* **5(2)** 122-137

[22] Kusano Y, Sørensen BF, Andersen TL and Leipold F 2013 *J. Adhesion* **89(6)** 433-459

[23] Kusano Y, Sørensen BF, Andersen TL, Toftegaard HL, Leipold F, Salewski M, Sun ZW, Zhu JJ, Li ZS and Aldén M 2013 *J. Phys. D Appl. Phys*. **46(13)** 135203

[24] Sun ZW, Zhu JJ, Li ZS, Aldén M, Leipold F, Salewski M and Kusano Y 2013 *Optics Express* **21(5)** 6028-6044

[25] Zhu JJ, Sun ZW, Li ZS, Ehn A, Aldén M, Salewski M, Leipold F and Kusano Y 2014 *J. Phys. D Appl. Phys*. **47**, 295203

[26] Kusano Y, Salewski M, Leipold F, Zhu JJ, Ehn A, Li ZS and Aldén M 2014 *Eur. Phys. J. D* **68** 319

[27] Kusano Y, Zhu JJ, Ehn A, Li ZS, Aldén M, Salewski M, and Leipold F 2015 *Surf. Eng*. **31(4)** 282-288

[28] Zhu JJ, Gao JL, Ehn A, Aldén M, Li ZS, Moseev D, Kusano Y, Salewski M, Alpers A, Gritzmann P and Schwenk M 2015 *Appl. Phys. Let*. **106** 044101

[29] Zhu JJ, Gao JL, Li ZS, Ehn A, Aldén M, Larsson A and Kusano Y 2014 *Appl. Phys. Let*. **105** 234102

[30] Peng BL, Dhar N, Liu HL and Tam KC 2011 *Canadian J. Chem. Eng*. **89(5)** 1191-1206

[31] Siqueira G, Tadokoro S K, Mathew AP and Oksman K 2016 *Comp. Sci. Technol*. **123** 49-56

[32] Bondeson D, Mathew AP and Oksman K 2006 *Cellulose* **13** 171-180

[33] Jonoobi M, Oladi R, Davoudpour Y, Oksman K, Dufresne A and Hamzeh Y 2015 *Cellulose* **22(2)** 935-969

[34] Nakagaito AN and Yano H 2005 *Appl. Phys. A* **80(1)** 155–159

[35] Herrera M, Mathew AP and Oksman K 2014 *Carbohydrate Polym*. **112** 494-501

[36] Herrera M, Sirviö J, Mathew A and Oksman K 2016 *Mater. Design* **93** 19-25

[37] Olsson RT, Azizi Samir MAS, Salazar-Alvarez G, Belova L, Ström V, Berglund LA, Ikkala O, Nogués J and Gedde UW 2010 *Nature Nanotechnol*. **5** 584-588

[38] Siró I, Kusano Y, Norrman K, Goutianos S and Plackett D 2013 *J. Adhesion Sci. Technol*. **27(3)** 294-308